Strong pinning linear defects formed at the coherent growth transition of pulsed-laser-deposited $YBa_2Cu_3O_{7-\delta}$ films

B. Dam, J. M. Huijbregtse, and J. H. Rector
Faculty of Sciences, Division of Physics and Astronomy, De Boelelaan 1081, NL-1081 HV, Amsterdam, The Netherlands
(Received 12 September 2001; published 23 January 2002)

Linear defects are important pinning sites for vortices in high-temperature superconductors. In $YBa_2Cu_3O_{7-\delta}$ thin films, the linear defects responsible for high critical currents are threading dislocations formed near the substrate interface. Investigating the first stages of growth of pulsed-lased-deposited $YBa_2Cu_3O_{7-\delta}$ on single terminated (100) $SrTiO_3$ substrates, we study the genesis of these dislocations. We find that the formation of linear defects occurs above a certain critical layer thickness at which a coherent growth transition takes place. Coherent islands are formed, surrounded by highly strained trenches. These trenches facilitate the formation of dislocation half-loops. Such half-loops relieve the misfit strain and form misfit and threading dislocations. The number of threading dislocations thus depends on the island density. This model explains both the short-range lateral order of the threading dislocations and their decreasing density at elevated substrate temperatures.

DOI: 10.1103/PhysRevB.65.064528 PACS number(s): 74.76.Bz, 74.60.Ge

I. INTRODUCTION

Recently, we showed that the presence of linear defects explains the high critical current density of $YBa_2Cu_3O_{7-\delta}$ thin films.[1] By wet-etching pulsed-laser-deposited (PLD) films in Br-ethanol we visualized the lateral distribution of (threading) linear defects. From the location of the etch pits we deduced that these linear defects are both edge and screw dislocations which, in PLD films, emerge mainly in the trenches between the growth islands. Indeed, *both* the growth island density and the threading dislocation density (n_{disl}) decrease when increasing the deposition temperature. Following the pattern of etch pits upon consequetive etching, we concluded that most threading defects originate from a region close to the interface.[2]

To uncover the mechanism by which these threading dislocations are formed, we address here the first stages of the PLD growth of $YBa_2Cu_3O_{7-\delta}$ thin films. In early experiments studying the heteroepitaxy of $YBa_2Cu_3O_{7-\delta}$ on (100) $SrTiO_3$ substrates, it was shown by reflective high-energy electron diffraction (RHEED) that this complex oxide grows unit cell by unit cell,[3] i.e., in blocks of 1.2 nm in height. As expected for mismatched heteroepitaxial systems, one observes relaxation of the film lattice at a critical layer thickness t_c of several monolayers.[4–6] Up to now, it was assumed that relaxation takes place by the introduction of misfit dislocations.[7] Yeadon *et al.*[8] estimated a (thermodynamic) critical layer thickness between 8 and 21 mm. This calculation is based on equating the strain energy to the energy of misfit relieving edge dislocations. However, misfit dislocations do not form spontaneously. Most probably, dislocation half-loops[8,9] have to nucleate at the film surface. The half-loop expands towards the interface where it forms a misfit dislocation and two *threading* dislocations ending at the film surface. The activation energy estimated for the initial halfloop formation is very high [between 30 and 100 eV (Ref. 10)]. Such a high activation energy in incompatible with the applied substrate temperature of 850 °C and with the fact that the threading defect density decreases with increasing growth temperature.[2] Hence we have to look for an alternative mechanism for the formation of misfit relieving and/or threading dislocations.

We investigated the structure and morphology during the first stages of growth of $YBa_2Cu_3O_{7-\delta}$ films, deposited on single terminated (100) $SrTiO_3$ substrates.[11] From atomic force microscopy (AFM) and x-ray diffraction (XRD) it appears that the defect structure of the initial growth layer depends strongly on the substrate termination. In particular, the critical thickness t_c up to which the film remains under epitaxial stress depends on the termination. Below t_c, the tetragonally distorted layer exhibits a kind of layer-by-layer growth, while relaxed islands start to grow above t_c, suggesting a Stranski-Krastanov type of growth mode. From our XRD data we infer that these surface ripples remain coherent with respect to the substrate. In analogy to what has been observed in heteroepitaxial semiconductor growth (see, e.g., the review by Mooney[12]), we propose that the relaxation into coherent islands reduces the activation energy for the nucleation of dislocation half-loops at the cusps between the islands (Fig. 1). These half-loops form misfit and threading dislocations. Hence, in PLD $YBa_2Cu_3O_{7-\delta}$ films, threading dislocations are preferentially found in the cusps between

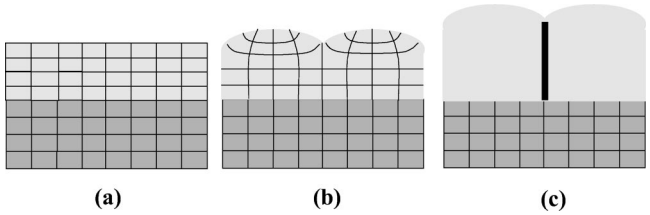

FIG. 1. Sketch of the first stages of growth: (a) pseudomorphic growth, the film adopts the lateral lattice constants of the substrate; (b) coherent islanding, the film relaxes by the formation of relaxed islands and strained trenches; and (c) dislocations form in the strained trenches between the coherent islands relieving (part of) the misfit strain.

growth islands.[2] As the island size is diffusion limited, the island density decreases when decreasing the substrate temperature. Hence our mechanism explains the paradox that an activated dislocation formation process produces less dislocations at high substrate temperatures. Moreover, it shows that the pinning properties of thin high-T_c films are intimately connected to the nucleation and growth process.

II. EXPERIMENTAL PROCEDURES

Low miscut, epi-polished (100) $SrTiO_3$ substrates are purchased from various suppliers. The $SrO/SiTiO_3$ termination is produced according to our *ex situ* procedure,[13] which consists of two essential steps. First, the as-received substrates are cleaned in 1-propanol under applying mechanical force and dried in air using a spinner. Second, the substrates are annealed in a quartz tube furnace, in flowing oxygen (0.5 l/min). The substrates are heated at 15 °C/min to 900 °C, annealed at this temperature for 5 h, and then cooled down (<15 °C/min). By studying the aging affects in air and the nucleation behavior of several (sub)monolayer thin films we have shown that the termination is different from the well-known $TiO_2/SrTiO_3$-terminated substrates and have a $SrO/SrTiO_3$ character.[13] $TiO_2/SrTiO_3$-terminated substrates are obtained commercially and are produced according to a modified[14] Kawasaki[15] procedure.

Thin films of $YBa_2Cu_3O_{7-\delta}$ are deposited on SrO- and TiO_2-terminated (100) $SrTiO_3$ substrates by means of pulsed laser deposition. Our PLD setup consists of a KrF excimer laser (LAMBDA PHYSIK LPX305: wavelength 248 nm, pulse duration τ=25 ns), projection optics, a beam-homogenizer, and a high-vacuum system with a base pressure below 10^{-5} Pa. The optical components ensure a spatially homogeneous laser spot on the target, essential to achieve high reproducibility.[16,17] The $YBa_2Cu_3O_{7-\delta}$ films are deposited from a rotating, polycrystalline, high-density, stoichiometric tetragonal target (PRAXAIR, >99.999>% pure raw materials) at an oxygen background pressure p_{O_2} = 15 Pa and a target-substrate distance $d_{T\text{-}S}$=3.5 cm. The laser energy density J is fixed at 1.4 J/cm^2, as measured at the target. Both the thickness t of the films and the substrate temperature T_{sub} are varied. We use three different substrate heater temperatures of T_{sub}=770, 805, and 850 °C, while t is varied from 0.8 nm up to 500 nm.

The surface morphology of both the $SrTiO_3$ substrates and the $YBa_2Cu_3O_{7-\delta}$ thin films is investigated by scanning probe microscopy (NANOSCOPE IIIa multimode system) in air. Atomic force microscopy measurements are performed in the tapping mode using Si tips. After deposition the surface morphology is immediately investigated by AFM in order to prevent degradation effects. The crystal structure of the films is investigated by x-ray diffraction and Rutherford backscattering spectrometry (RBS). The 10 kW Rigaku rotating-anode XRD employs Cu $K\alpha$ radiation in line focus. This two-circle diffractometer is equipped with secondary optics only, consisting of a Soller slit and a graphite monochromator. Two sets of XRD experiments are performed. Radial (θ-2θ) scans are recorded in order to measure the length of the c-axis lattice parameter. For the ultrathin films, the scans were limited to the 005 and 001 reflection mostly. Second, longitudinal (ω) scans are performed for the 00l reflections (l=1–10), mostly the 005 only. The resolution in these rocking scans is about 0.04°, as estimated by measuring a Si wafer.

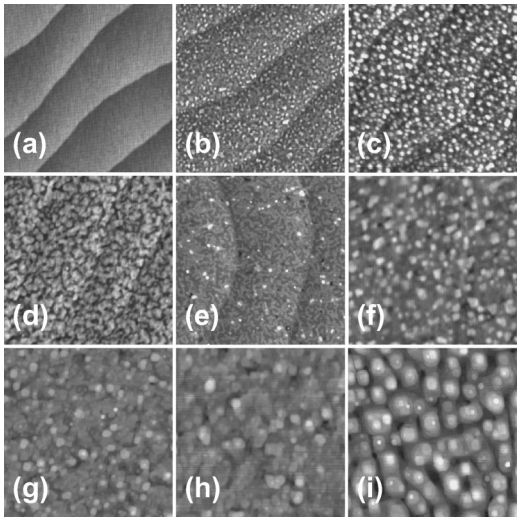

FIG. 2. 1.0×1.0 μm^2 AFM height images of $YBa_2Cu_3O_{7-\delta}$ films pulsed laser deposited at T_{sub}=805 °C on TiO_2-terminated (100) $SrTiO_3$ as a function of film thickness t: (a) bare substrate, (b) t=0.8 nm, (c) t=1.6 nm, (d) t=2.4 nm, (e) t=3.2 nm, (f) t=4.1 nm, (g) t=8.1 nm, (h) t=16.2 nm, and (i) t=24.3 nm. The height scales are (a–e) 5.0 nm, (f) 7.5 nm, (g) 15.0 nm, and (h,i) 20 nm, respectively; identical image conditions (contrast, color table, etc.) are used.

III. RESULTS

A. Surface morphology

Using AFM we compared the surface morphology of films deposited on both substrate terminations as a function of film thickness t. The results for 0.8<t<24.3 nm are summarized in Figs. 2 and 3. For all $YBa_2Cu_3O_{7-\delta}$ films deposited at T_{sub}=805 °C we distinguish three main growth stages.

(i) *Nucleation stage.* The films nucleate precipitate free on $TiO_2/SrTio_3$, while a high density of precipitates forms on $SrO/SrTiO_3$. This behavior originates from non-unit-cell nucleation and has been observed before.[13,18,19] In complex oxides, the stability of the nucleation layer is a complicated balance between interface, surface, edge, and strain energies. Under our growth conditions we find that, in contrast to, e.g., a 122 monolayer, a single 123 monolayer is unstable on $SrO/SrTiO_3$. CuO precipitates are formed instead.[13]

(ii) *Two-dimensional growth.* Surprisingly, when growing slightly thicker films, we no longer observe the precipitates. They have apparently dissolved in the growing film. Growth proceeds in a kind of layer-by-layer mode. Nucleation and growth of unit-cell layers of $YBa_2Cu_3O_{7-\delta}$ can be discerned [e.g., Figs. 2(c)–2(f), Figs. 3(c)–3(f)]. Nucleation is random, and preferred nucleation sites cannot be discerned. In this stage probably the RHEED oscillations[20,21] are observed. On

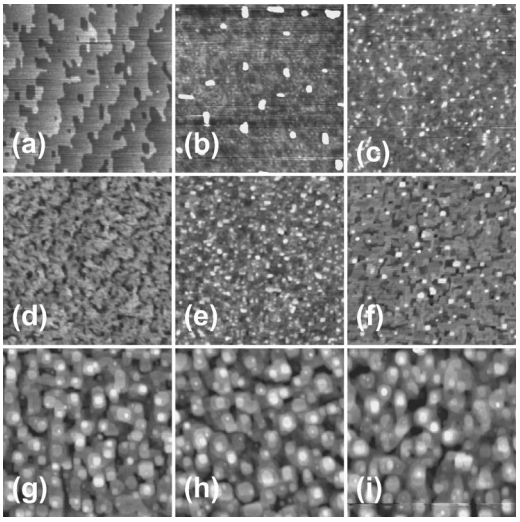

FIG. 3. 1.0×1.0 μm^2 AFM height images of $YBa_2Cu_3O_{7-\delta}$ films pulsed laser deposited at $T_{sub}=805$ °C on SrO-terminated (100) $SrTiO_3$ as a function of film thickness t: (a) bare substrate, (b) $t=0.8$ nm, (c) $t=1.6$ mm, (d) $t=2.4$ nm, (c) $t=3.2$ nm, (f) $t=4.1$ nm, (g) $t=8.1$ nm, (h) $t=11.3$ nm, and (i) $t=16.2$ nm. The height scales are (a)–(e) 5.0 nm, (f) 7.5 nm, (g),(h) 15.0 nm, and (i) 20 nm, respectively; identical image conditions (contrast, color table, etc.) are used.

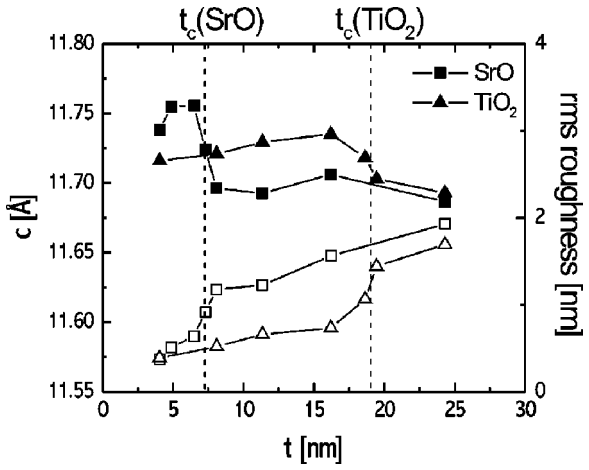

FIG. 4. c-axis length (solid symbols) of laser-ablated $YBa_2Cu_3O_{7-\delta}$ films on SrO- and TiO_2-terminated (100) $SrTiO_3$ as a function of film thickness t. The drop in c is accompanied by the morphological transition, as indicated by the AFM root-mean-square roughness (open symbols). The transition thickness t_c shifts to higher values when depositing films at lower T_{sub}.

$TiO_2/SrTiO_3$ the vicinal steps are reproduced by the $YBa_2Cu_3O_{7-\delta}$ layers [i.e., at these steps antiphase boundaries (APB's) are created] up to a thickness of around $t=11$–16 nm. On the SrO-terminated substrate, steps cannot be discerned after the second $YBa_2Cu_3O_{7-\delta}$ monolayer. This implies that the film has quickly accommodated to the average substrate orientation. We assume that the stacking faults required for such a lattice tilt form out of the dissolved secondary phases.

(ii) *Island growth.* At a critical thickness, the relatively flat surface morphology suddenly changes into the island structure that is well known from thicker $YBa_2Cu_3O_{7-\delta}$ films. Nucleation is not random anymore, but results in concentric steps. Remarkably, the critical layer thickness of the morphological transition on SrO-terminated $SrTiO_3$ ($t_c^{SrO}=6.9$ nm) is much smaller compared to the TiO_2/$SrTiO_3$ termination ($t_c^{TiO_2}=19$ nm). The island density is approximately the same for both terminations.

The initial layer-by-layer growth indicates that the attachment of the film to the substrate is stronger than the attachment energy of growth units within the film. As the strain energy of the film increases with its thickness, relaxation at a certain thickness is to be expected. This is typical for Stranski-Krastanov growth, be it incoherent or coherent.[22] To our knowledge, a termination dependence of the critical thickness has never been observed before. In the case of an incoherent growth transition the surface morphology is characterized by a gridlike surface morphology,[23] which is related to the formation of misfit dislocations. In case of a coherent growth transition, islands (surface ripples) are formed which allow for a release of the lateral strain by lattice bending. The island structure we observe above t_c suggests that we are dealing with such a coherent relaxation.[25]

B. Crystal structure

1. Relaxation of the c axis

We measure the 005 reflection as a function of film thickness and temperature on both substrate terminations by performing θ-2θ scans. From the peak position we determine the c-axis length for all films. We calculate the film thickness t from the frequency of the Laue oscillations around the 001 reflection.[26] In Fig. 4 the measured c axis is shown as a function of film thickness for the two terminations for the intermediate substrate temperature of 805 °C.

Surprisingly, on both terminations initially we find an enlarged c axis (11.72–11.75 Å), which suddenly drops to a more bulklike value [$c=11.6772$ Å (Ref. 27)] at $t>t_c$. Actually, one would expect a reduced c axis below t_c. Initially, the film is under tensile strain as a result of the larger substrate lattice. This should cause a Poisson contraction of the c axis. How can we explain the enlarged c axis? As the films grow in the *tetragonal* phase (with lattice constants[27] of 3.8578 Å in plane and 11.8391 Å out of plane), Fig. 4 implies that the transformation into the orthorhombic form upon cooling down only occurs above t_c. Due to strain, thinner overlayers remain tetragonal $YBa_2Cu_3O_{6+x}$.[28] As a result of the larger lattice constant of the substrate (3.905 Å), for $t<t_c$ the c axis is contracted with respect to its tetragonal value. As we lower the substrate temperature, t_c shifts to larger values for lower temperatures (from 6.5 nm at 850 °C to 8.0 nm at 770 °C for films on $SrO/SrTiO_3$). Similarly as in thicker films,[2] the island size increases with temperature.

The simultaneous structural relaxation and formation of islands (evidenced by a jump in the surface roughness as

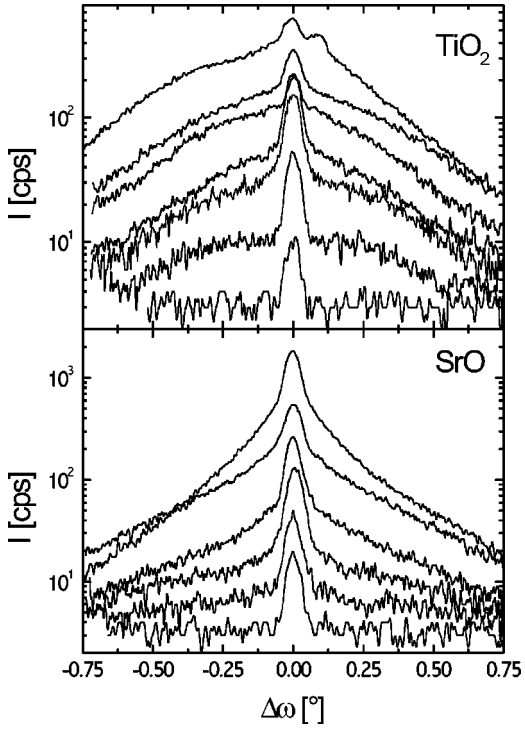

FIG. 5. 005 rocking curves (ω scans) of laser-ablated $YBa_2Cu_3O_{7-\delta}$ films as a function of film thickness t and (100) $SrTiO_3$ termination: (top) t=3.2, 4.1, 8.1, 11.3, 16.2, 18.6, and 24.3 on $TiO_2/SrTiO_3$ and (bottom) t=3.2, 4.1, 6.5, 8.1, 16.2, and 24.3 nm on $SrO/SrTiO_3$; t increases from bottom to top.

plotted in Fig. 4) are to be expected for a coherent, *pseudomorphic* growth transition. We do not known whether the island formation takes place through a rearrangement of the film surface layers or through a clustering process during growth. In any case, the different t_c for the two terminations indicates that the roughening is not due to some trivial thickness dependence of the growth kinetics.

2. Defect structure and the in-plane order

Unfortunately, we could not verify the relaxation of the in-plane lattice parameters, as only 001 reflections were sufficiently strong to be observed. However, 001 rocking curves reflect important information on the lattice perfection of thin films. Rocking curves (ω scans) were taken around the 005 reflection as a function of the film thickness (Fig. 5). The rocking curves of the ultrathin $YBa_2Cu_3O_{7-\delta}$ on both the SrO- and TiO_2-terminated (100) $SrTiO_3$ substrates initially exhibit *two* components: a narrow (specular) resolution-limited component and a broader (diffuse) component. On $TiO_2/SrTiO_3$ the diffuse component has a Gaussian profile, whereas it has a Lorentian shape on $SrO/SrTiO_3$. In Fig. 6 the full width at half maximum (FWHM) of the broad and narrow components are plotted as a function of the film thickness, as determined by fitting an appropriate two-component peak function. It follows that the FWHM of the narrow component is mainly determined by the instrumental resolution, although a slight increase with t can be detected. On the other hand, the FWHM of the broad component decreases rapidly with film thickness, roughly linear in the films on $TiO_2/SrTiO_3$-terminated substrates, while on $SrO/SrTiO_3$ the decrease is more exponential. To investigate the temperature dependence of the two component rocking curves, we deposited ultrathin films on $SrO/SrTiO_3$ at a substrate temperature of 770 and 850 °C. It appeared that the FWHM of both the broad and narrow components is remarkably insensitive to the substrate temperature.

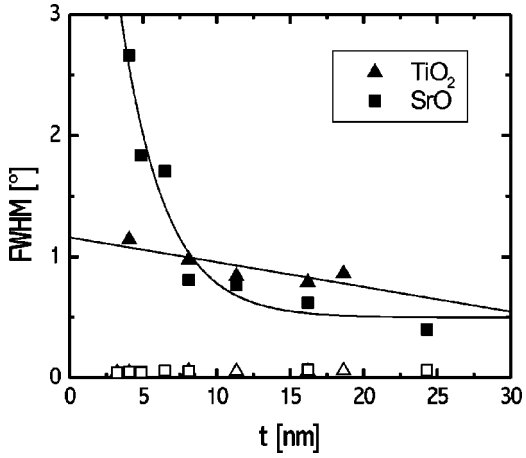

FIG. 6. Full width at half maximum (FWHM) of the broad and narrow (open symbols) components of the 005 rocking curves of $YBa_2Cu_3O_{7-\delta}$ films on TiO_2- and SrO-terminated (100) $SrTiO_3$ as a function of film thickness t.

In many heteroepitaxial systems similar diffraction features have been observed—for instance, in ErAs/GaAs (Ref. 29) and Nb on sapphire (Ref. 30). The narrow component, especially when it is visible in higher-order Bragg reflections, is usually interpreted as resulting from perfectly aligned epitaxial film regions, whereas the diffuse component is due to incoherent scattering due to defects.[31–33] These theories consider misfit dislocations as the most important source of diffuse scattering. The intensity of the sharp component is inversely related to the misfit dislocation density in the case of weak disorder, i.e., in the regime for which the product of the dislocation density and the film thickness $pt<1$.[33] For ultrathin $YBa_2Cu_3O_{7-\delta}$ films this is the case, even in the fully relaxed state, i.e., with a misfit dislocation spacing of 40 nm. Unfortunately, the resolution of our system is insufficient to quantitatively compare the fraction of the specular and the diffuse intensity. However, Fig. 5 clearly shows no anomalous decrease in the specular reflection around t_c. Remarkably, the specular reflection remains easily visible in up to 24 nm thin films, from which we conclude that most of them is fit dislocations yet have to be formed.

To further analyze the nature of the diffuse scattering we recorded 00l rocking curves for l in the range from 1 up to 10. In Fig. 7 the result is shown for the 16.2 nm film deposited at 770 °C on SrO-$SrTiO_3$. The normalized intensity plotted versus the parallel scattering vector $q_p = (4\pi/\lambda)(\cos\theta_0 - \cos\omega)$ does not depend on the order of the reflection, characteristic for a small correlation length. On the other hand, the 00l rocking curves for a 165-nm-thick film show a constant lateral width in angle space, indicative of rotational disorder. At this thickness the specular

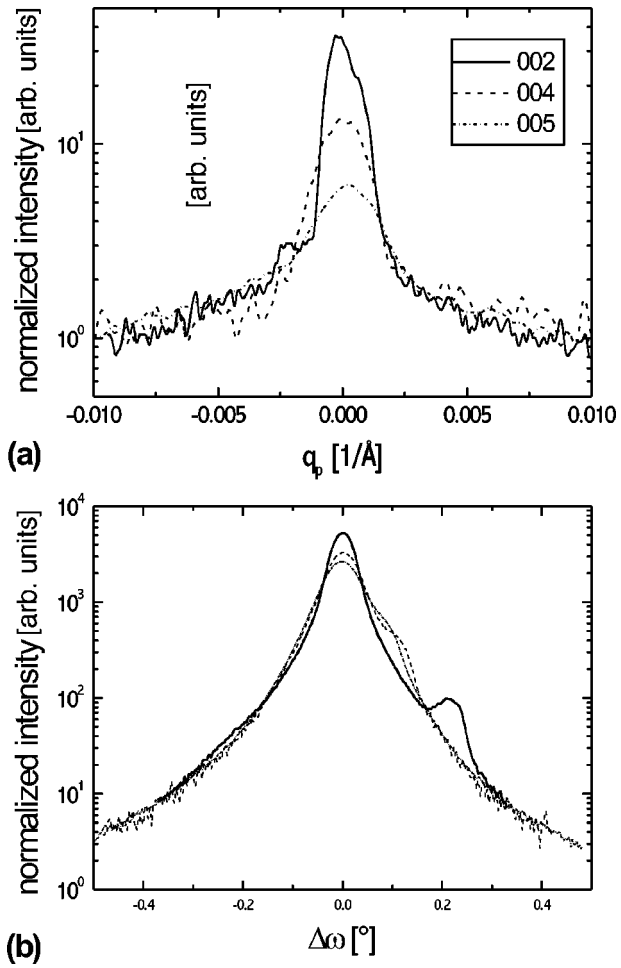

FIG. 7. Normalized 005 rocking curves (ω scans, $l=2$, 4, and 5) of $YBa_2Cu_3O_{7-\delta}$ films on SrO-terminated (100) $SrTiO_3$: (a) a 16.2 nm thin film shows a constant width of the broad component in reciprocal space, characteristic for a small correlation length, while (b) a 165 nm thick film shows a fixed width in angle space, indicative of rotational disorder. Specular scattering is not observed.

peak has disappeared. Miceli *et al.*[32] attributed such a cross over in ErAs films to the introduction of misfit dislocations. In very thin films no strain relaxation occurs and strong specular scattering is observed even for large *l*. The diffuse scattering is correlation length limited and hence the width of the broad component does not depend on the order of the reflection when plotted against the parallel scattering vector. In thicker films, misfit dislocations at the interface relieve the mismatch strain and the strong disorder limit applies. In this limit, only weak specular scattering (decreasing with *l*) is expected, while the diffuse component is purely rotational in character and therefore (as we observe) has a constant width in angle space. Accordingly, we propose that (most) misfit dislocations are formed at layer thicknesses above 24 nm.

Since the model of Miceli *et al.* only predicts the *width* of the broad reflection and not its line shape (except in the weak order limit when the displacement fields are very small), we attribute the different line shapes of the broad component (Lorentzian on SrO- and Gaussian on TiO_2/$SrTiO_3$-terminated substrates) to a different type defect structure on both terminations. Given our morphological observations, we expect different densities of, e.g., APB's and stacking faults to be the cause of the different line shapes.

IV. DISCUSSION

A. Coherent growth transition

The Stranski-Krastanov growth mode is characterized phenomenologically by the formation of islands on a thin wetting layer. It results from the competition between the interface energy (which has a finite range) and the misfit strain energy which increases with layer thickness.[34] Depending on temperature and strain[35] the relaxation proceeds incoherently (immediate formation of misfit dislocations) or coherently (misfit dislocations form in a later growth stage). In the latter case a surface ripple structure forms, which precedes the formation of the isolated islands. The coherent islands can be quite uniform in size and lateral distribution. Currently, these so-called self-assembled quantum dots (SAQDs) have received a lot of attention because of their interesting electronic properties.

The islands we observe can be characterized as a surface ripple structure. Although the surface area increases, the ripple formation allows for a partial relaxation of the strain by elastic deformation of the film surface. The roughening may take the form of sharp pits or grooves,[36] at which the stress is concentrated resulting in a locally reduced barrier for the nucleation of dislocations.[37,38] The formation of surface ripples requires an activation energy. The activation energy barrier occurs at a critical nucleus size, which depends on both the film surface energy and the misfit-induced strain.[35] For the size of the islands, a critical wavelength λ_{cr} has been defined[24] above which the ripples are thermodynamically stable:

$$d/\lambda_{cr}^2 = C\varepsilon^2/4\gamma\pi^2. \tag{1}$$

Here d is the amplitude of the undulation, C is Young's modulus, γ is the surface free energy of the film, and ε is the mismatch strain. Assuming 1.6 J/m^2 for the surface free energy of $YBa_2Cu_3O_{7-\delta}$,[7] we find that the island shape we observe (3×100 nm) is of the required order of magnitude. While Eq. (1) suggests only a small dependence of the critical wavelength on temperature, the actual increase can be quite large (a factor of 2–5). We attribute this to an increased diffusivity, which is known to have a strong influence on the actual island size (see Gao and Nix[39]). Also, the time for the formation of the ripple structure depends on the diffusivity, which explains the temperature dependence of t_c. Note that these theories refer to the surface evolution of a film during annealing. It would be interesting to perform an anneal experiment on unrelaxed films. However, such an experiment is hampered by the fact that the background oxygen pressure required for the phase stability also has a profound effect on the diffusivity.

As far as we know, a termination dependence of the critical thickness has not been observed before in a (coherent)

Stranski-Krastanov (SK) transition. In general, in the SK-growth mode, islands form on top of an unperturbed wetting layer. The thickness of the wetting layer depends on the interface energy,[40] which depends on the exact nature of the interface. The energy per unit area of a pseudomorphic layer *A* of thickness *t* deposited on a substrate (material B) may be written as

$$E(t)=(C\varepsilon^2-\Phi_{AA})t+W+S. \tag{2}$$

In this approach[41] C is Young's modulus, $\varepsilon=0.012$ equals the substrate-film mismatch, Φ_{AA} is the binding energy of an unperturbed film, *W* sums the interaction of all layers with the substrate, and *S* equals the surface energy of the film. Since the surface energy of the film itself is not expected to depend on the type of interface, we may attribute the differences in t_c to the difference in *W*. Assuming that the energy of the pseudomorphic layer at the critical thickness t_c is the same for both terminations,

$$(W_{\mathrm{TiO_2}}-W_{\mathrm{SrO}})=(C\varepsilon^2-\Phi_{\mathrm{YBCO}})(t_c^{\mathrm{TiO_2}}-t_c^{\mathrm{SrO}}). \tag{3}$$

We estimate that the upper limit for the difference in substrate interaction energy equals $(W_{\mathrm{TiO_2}}-W_{\mathrm{SrO}})=0.39$ J/m^2. Basically, this implies a termination-dependent wetting layer thickness. A wetting layer thickness of over 10 nm seems, however, a bold suggestion.

Alternatively, the difference in t_c could be due to the different stiffness of the initial growth layers. As the defect structure of the film depends on the substrate termination, the effective Young's modulus will be affected also. As the strain energy is the driving force for the coherent relaxation, a high defect density ($SrO/SrTiO_3$ termination) implies a higher strain energy density. As a result, the activation energy for island formation decreases,[35] along with the critical layer thickness.

B. Implications for the formation of threading dislocations

Below t_c, we do not observe any morphological indication for the formation of defects. In contrast to what was observed by, e.g., Bauer *et al.* on MgO,[42] we do not observe any signs of incoherent growth fronts forming screw dislocations. Moreover, from our diffraction data we conclude that at t_c, only very few misfit dislocations have formed. As a result, the trenches between the coherent islands are highly strained.[24] In our view the local strain facilitates the formation of threading dislocations, e.g., by the nucleation of dislocation half-loops. Calculations show that the activation energy for dislocation half-loop formation is dramatically reduced in such cusps.[37,38] As a result, when growing beyond t_c, dislocations may form that release (part of the) misfit strain. Indeed, in PLD $YBa_2Cu_3O_{7-\delta}$ films ($50<t<500$ nm) the threading dislocations are always found to emerge at the trenches between the growth islands, leading to an average dislocation density equal to the island density.[2] The fact that the trenches remain present in thicker films indicates that not all strain is released. The reduction of the threading dislocation density with substrate temperature follows from the decrease in island density in the first stages of growth.[43]

So far, we have neglected the nature of the threading dislocation and the effect of the growth technique on the dislocation formation. Typically, depending on the growth conditions,[44] in PLD the $YBa_2Cu_3O_{7-\delta}$ islands grow in a two-dimensional nucleation and growth mode and we cannot distinguish between edge and screw dislocations. On sputtered films[45,46] growth spirals are observed in the *middle* of the growth islands. These spirals reveal the presence of screw dislocations. To understand that growth spirals are not seen in the trenches, one has to take into account the effect of growth kinetics. If (under the proper growth conditions) screw dislocations form growth spirals, these dislocation outcrops become step sources. The spiral will become the center of a growth island, filling up the trench. Edge dislocations never act as step sources. As a result, these cusps remain intact. It is reasonable to assume the same coherent growth transition in sputtered films as in PLD-grown films. We predict, however, that due to the formation of growth spirals, the island density of sputtered films is less than that of corresponding PLD films.

The observation of growth spirals indicates that the Burgers vector of many threading dislocations has a screw component. If threading dislocations are part of a misfit relieving dislocation half-loop, they must have an edge component also. Experimentally, the nature of the threading dislocations is still under debate. Transmission electron microscopy (TEM) observations remained inconclusive,[8,47] but do not exclude the predominance of mixed dislocations. Note that a thick film is usually fully relaxed, implying a misfit dislocation density higher than the threading dislocation density. The formation mechanism of these additional misfit dislocations is not clear.[48]

At first sight our reasoning implies that the dislocation density (although not affected by the substrate termination) should depend strongly on the substrate chosen. Indeed, Svetchnikov *et al.*[49] report anomalously high dislocation densities in $YBa_2Cu_3O_{7-\delta}$ grown on MgO (which has a lattice mismatch of 9%). However, partly this may be due to the 45° grain boundaries. On single grains, we find basically the same threading dislocation density on MgO as on $SrTiO_3$.[2] The low threading dislocation density on MgO can be understood following a suggestion from Yeadon *et al.*[8] They find that on MgO the $YBa_2Cu_3O_{7-\delta}$ growth mode is of Volmer-Weber (VW) type (i.e., relaxed islands form immediately in the initial growth stage). They claim that the VW islands have a residual misfit of the same order of magnitude as that of films grown on $SrTiO_3$. Hence the same type of relaxation might also occur within these growth islands. Further investigation of the growth and defect formation on $YBa_2Cu_3O_{7-\delta}$ on different substrates would be worth pursuing.

At this stage we can only speculate on the applicability of our dislocation formation model to other high-T_c films or complex oxides in general. The typical island morphology is, e.g., not seen on $Bi_2Sr_2CaCu_2O_x$ compounds. The lower misfit and the higher surface free energy may in this case prevent the coherent island formation. A detailed study of the defect structure of complex oxides is necessary to judge how far the analogy with semiconductors holds.

V. CONCLUSIONS

In the first stages of the PLD growth of $YBa_2Cu_3O_{7-\delta}$ films on single terminated (100) $SrTiO_3$, we observe layer-by-layer growth by random nucleation. The films remain remarkably flat, until they roughen at a critical layer thickness (t_c). Remarkably, we find that t_c depends strongly on the substrate pretreatment, i.e., the substrate surface termination. The roughening therefore is not a trivial effect of the layer thickness alone. As we find no morphological or structural evidence for the formation of misfit dislocations, we conclude that t_c is determined by a coherent growth transition.

The features observed in the first stages of the heteroepitaxy of $YBa_2Cu_3O_{7-\delta}$ on (100) $SrTiO_3$ imply the following model for the generation of (strong pinning) threading dislocations parallel to the growth direction in PLD-grown $YBa_2Cu_3O_{7-\delta}$ films (see also Fig. 1).

(1) Up to a critical layer thickness t_c, the film grows by random nucleation. The surface roughness is limited to plus or minus one monolayer.

(2) Upon reaching t_c, misfit strain is released by the formation of coherent islands. The minimal size of these islands is determined by the balance between surface and strain energy. The actual size of the islands is increased due to the surface mobility. As a result, when increasing the deposition temperature the island density decreases.

(3) Growing beyond t_c induces the formation of dislocation halfloops in the trenches between the coherent islands. Due to the strain concentrated there, trenches are preferred sites for half-loop formation. Dislocation half-loops extend to form misfit dislocations at the interface and threading dislocations along the growth direction.

(4) The island density depends hardly on the layer thickness.[43] As a result, the dislocation density is proportional to the island density. The island density decreases at elevated substrate temperatures, due to the increased surface mobility at t_c.

The dependence of the critical layer thickness t_c on the substrate termination is somewhat elusive. It illustrates the complexity of the heteroepitaxial growth of complex oxides, which are characterized by long-range ionic bonds and ambiguous interface configurations.

In high-T_c superconductors we want to have as many dislocations as possible. Preferably, the dislocation should be laterally ordered. Moreover, the dislocations should not affect the quality of the surrounding superconductor.[1] In the single-vortex pinning regime, strong pinning induces the superconducting critical current to remain constant up to a matching field, which is proportional to the density of threading defects. We expect (especially due to the growth induced lateral ordering) that we can extend the critical current plateau to above 1 T if we could, e.g., force a 1:1 correlation between misfit and threading dislocations. To achieve that a further investigation into the nature of coherent islands and the associated defect formation in heteroepitaxial films of complex oxides is needed.

Note that while semiconductor research focuses on the prevention of threading dislocations, in superconductors these defects are necessary to obtain high critical currents. On the other hand as has been shown by Locquet *et al.*,[50] the strain in the coherent state can be used to increase T_c in $La_{1.9}Sr_{0.1}CuO_4$ thin films.

ACKNOWLEDGMENTS

This work is part of the research program of FOM (stichting Fundamenteel Onderzoek der Materie), which is financially supported by NWO (stichting Nederlands Wetenschappelijk Onderzoek).

[1] B. Dam, J. M. Huijbregtse, F. C. Klaassen, R. C. F. van de Geest, G. Doornbos, J. H. Rector, A. M. Testa, S. Freisem, J. C. Martinez, B. Stäuble-Pümpin, and R. Griessen, Nature (London) **399**, 439 (1999).

[2] J. M. Huijbregtse, B. Dam, R. C. F. van der Geest, F. C. Klaassen, R. Elberse, J. H. Rector, and R. Griessen, Phys. Rev. B **62**, 1338 (2000).

[3] T. Terashima, Y. Bando, K. Iijima, K. Yamamoto, K. Hirata, K. Hayashi, K. Kamigaki, and H. Terauchi, Phys. Rev. Lett. **65**, 2684 (1990).

[4] T. Terashima, K. Iijima, K. Yamamoto, K. Hirata, Y. Bando, and T. Takada, Jpn. J. Appl. Phys., Part 2 **28**, L987 (1989).

[5] A. Abert, J. P. Contour, A. Dfossez, D. Ravelosona, W. Schwegle, and P. Ziemann, Appl. Surf. Sci. **96-98**, 703 (1996).

[6] M. Bauer, F. Baudenbacher, and H. Kinder, Physica C **246**, 113 (1995).

[7] D. G. Schlom, d. Anselmetti, J. G. Bednorz, R. F. Broom, A. Catana, T. Frey, Ch. Gerber, H.-J. Günterodt, H. P. Lang, and J. Mannhart, Z. Phys. B: Condens. Matter **86**, 163 (1992).

[8] M. Yeadon, M. Aindow, F. Wellhofer, and J. S. Abell, J. Cryst. Growth **172**, 145 (1997).

[9] S. J. Pennycook, M. F. Chisolm, D. E. Jesson, R. Feenstra, S. Zhu, X. Y. Zheng, and D. J. Lowndes, Physica C **202**, 1 (1992).

[10] B. Stäuble-Pümpin, V. C. Matijasevic, B. Ilge, J. E. Mooij, W. J. A. M. Peterse, P. M. L. O. Scholte, F. Tuinstra, H. J. Venvik, D. S. Wai, C. Traeholt, J. C. Wen, and H. W. Zandbergen, Phys. Rev. B **52**, 7604 (1995); B. Stäuble-Pümpin (private communication).

[11] Tsuyoshi Ohnishi, Kazuhiro Takahashi, Massashi Nakamura, Masashi Kawasaki, Mamoru Yoshimoto, and Hidcomi Koinuma, Appl. Phys. Lett. **74**, 2531 (1999).

[12] P. M. Mooney, Mater. Sci. Eng., R. **17**, 105 (1996).

[13] J. M. Huijbregtse, J. H. Rector, and B. Dam, Physica C **351**, 183 (2001).

[14] Gertjan Koster, Boike L. Kropman, and Guus J. H. M. Rijnders, Appl. Phys. Lett. **73**, 2920 (1998).

[15] Masashi Kawasaki, Kazuhiro Takahashi, Tatsuro Maeda, Ryuta Tsuchiya, Makoto Shinohara, Osamu Ishiyama, Takuza Yonezawa, Mamoru Yoshimoto, and Hideomi Koinuma, Science **266**, 1540 (1994).

[16] B. Dan, J. Rector, M. F. Chang, S. Kars, D. G. de Groot, and R. Griessen, Appl. Phys. Lett. **65**, 1581 (1994).
[17] J. M. Huijbregtse, B. Dam, J. H. Rector, and R. Griessen, J. Appl. Phys. **86**, 6528 (1999).
[18] J. G. Wen, T. Morishita, N. Koshizuka, C. Traeholt, and H. W. Zandbergen, Appl. Phys. Lett. **66**, 1830 (1995).
[19] V. C. Matijasevic, B. Ilge, B. Stäuble-Pümpin, G. Rietveld, F. Tuinstra, and J. E. Mooij, Phys. Rev. Lett. **76**, 4765 (1996).
[20] D. G. Schlom, D. Anselmetti, J. H. Bednorz, Ch. Gerber, and J. Mannhart, J. Cryst. Growth **137**, 259 (1994).
[21] Guus J. H. M. Rijnders, Gertjan Koster, Dave H. A. Blank, and Horst Rogalla, Appl. Phys. Lett. **70**, 1888 (1997).
[22] G. H. Gilmer, Hanchen Huan, and Christopher Roland, Comput. Mater. Sci. **12**, 354 (1998).
[23] M. A. Lutz, R. M. Feenstra, P. M. Mooney, J. Tersoff, and J. O. Chu, Surf. Sci. **316**, L1075 (1994).
[24] A. G. Cullis, MRS Bull. **21**, 21 (1996).
[25] C. W. Snyder, B. G. Orr, D. Kessler, and L. M. Sander, Phys. Rev. Lett. **66**, 3032 (1991); C. W. Snyder, J. F. Mansfield, and B. G. Orr, Phys. Rev. B **46**, 9551 (1992).
[26] W.-J. Lin, P. D. Hatton, F. Baudenbacher, and J. Santiso, Appl. Phys. Lett. **73**, 2995 (1998).
[27] F. S. Galasso, *Perovskites and High T_c Superconductors* (Gordon and Breach, New York, 1990).
[28] See, for instance, K. Kamigaki, H. Teauchi, T. Terashima, Y. Bando, K. Iijam, K. Yamamoto, K. Hirata, K. Hayashi, I. Nakagawa, and Y. Tomii, J. Appl. Phys. **68**, 3653 (1991); Q. D. Jiang, D.-M. Smilgies, R. Feidenhans'l, M. Cardona, and J. Zegenhagen, Solid State Commun. **98**, 157 (1996); A. del Vecchio, M. F. de Riccardis, L. Tapfer, C. Camerlingo, and M. Russo, J. Vac. Sci. Technol. A **18**, 802 (2000).
[29] P. F. Miceli, C. J. Palstrøm, and K. W. Moyers, Appl. Phys. Lett. **58**, 1602 (1991).
[30] P. M. Reimer, H. Zabel, C. P. Flynn, and J. A. Dura, Phys. Rev. B **45**, 11 426 (1992).
[31] P. Kidd, P. F. Fewster, and N. L. Andrew, J. Phys. D **28**, A133 (1995).
[32] P. F. Miceli and C. J. Palstrøm, Phys. Rev. B **51**, 5506 (1995); P. F. Micelli, J. Weatherwax, T. Krentsel, and C. J. Palstrøm, Physica B **221**, 230 (1996).
[33] V. M. Kaganer, R. Köhler, M. Schmidbauer, and R. Opitz, Phys. Rev. B **55**, 1793 (1997).
[34] R. J. Asaro and W. A. Tiller, Metall. Trans. A **3**, 1789 (1972).
[35] J. Tersoff and F. K. LeGoues, Phys. Rev. Lett. **72**, 3570 (1994).
[36] W. H. Yang and D. J. Srovolitz, Phys. Rev. Lett. **71**, 1593 (1993).
[37] D. E. Jenson, S. J. Pennycook, J.-M. Baribeau, and D. C. Houghton, Phys. Rev. Lett. **71**, 1744 (1993).
[38] A. G. Cullis, A. J. Pidduck, and M. T. Emeny, Phys. Rev. Lett. **75**, 2368 (1995).
[39] Huajian Gao and William D. Nix, Annu. Rev. Mater. Sci. **29**, 173 (1999).
[40] I. Duraka and A.-L. Barabási, Phys. Rev. Lett. **79**, 3708 (1997).
[41] V. A. Shchukin and D. Bimberg, Rev. Mod. Phys. **71**, 1125 (1999).
[42] M. Bauer, F. Baudenbacher, and H. Kinder, Physica C **246**, 113 (1995).
[43] J. M. Huijbregtse, Ph.D. thesis, Vrije Universiteit Amsterdam, 2001; J. M. Huijbregtse, F. C. Klaassen, A. Szepielow, B. Dam, and R. Griessen, Supercond. Sci. Technol. **15**, 1 (2002).
[44] B. Dam, J. H. Rector, J. M. Huijbregtse, and R. Griessen, Physica C **305**, 1 (1998).
[45] M. Hawley, I. D. Raistrick, J. B. Beery, and R. J. Houlton, Science **251**, 1587 (1991).
[46] Ch. Gerber, D. Anselmetti, J. G. Bednorz, J. Mannhart, and D. G. Schlom, Nature (London) **350**, 279 (1991).
[47] O. Eibl and B. Roas, J. Mater. Res. **5**, 2620 (1920).
[48] R. Beanland, J. Appl. Phys. **77**, 6217 (1995).
[49] V. Svetchnikov, V. Pan, C. Traeholt, and H. Zandbergen, IEEE Trans. Appl. Supercond. **7**, 1396 (1997).
[50] J.-P. Locquet, J. Perret, J. Fompeyrine, E. Maechler, J. W. Seo, and G. van Tendeloo, Nature (London) **393**, 453 (1998).